Inorganic Chemistry
Article

Inorg. Chem. **2009**, *48*, 9427–9435 **9427**
DOI: 10.1021/ic901319n

Synthesis, Structural Characterization, and Quadruplex DNA Binding Studies of Platinum(II)-Terpyridine Complexes

Kogularamanan Suntharalingam, Andrew J. P. White, and Ramon Vilar*

Department of Chemistry, Imperial College London, London SW7 2AZ, U.K.

Received July 8, 2009

Three new substituted terpyridine ligands and their corresponding platinum(II) complexes have been prepared and fully characterized (including the X-ray crystal structures of two of the complexes). These compounds have shown to stack via $\pi-\pi$ interactions both in the solid state and in solution. The interactions of these compounds with quadruplex DNA (both *HTelo* and *c-myc* sequences) have been studied by fluorescent indicator displacement (FID) assays, surface plasmon resonance (SPR), and in one case by circular dichroism (CD). The complexes have shown to interact strongly with quadruplex DNA (with binding constants of ca. 10^6 and DC_{50} values between 2.24 and 0.26, as determined by SPR and FID, respectively). We have also investigated the interaction between the complexes and a sequence of duplex DNA to gain some insight into the selectivity of the compounds for quadruplex structures. FID and SPR studies have shown that the complexes have a modest selectivity (1 order of magnitude) for quadruplex, particularly *c-myc*, versus duplex DNA.

Introduction

Guanines have the ability to assemble into planar molecular squares via hydrogen-bonding interactions between the Watson−Crick edge of one guanine and the Hoogsteen edge of its neighbor (see Figure 1).[1] These structures can be further stabilized by the presence of alkali metal cations (e.g., potassium or sodium) which interact electrostatically with the guanines' carbonyl groups. Thus, guanine-rich sequences of DNA can yield several of these guanine tetrads which in turn can stack via $\pi-\pi$ interactions generating quadruplex DNA structures (see Figure 1b for a schematic representation). Recently, bioinformatic studies have shown that in the human genome there are approximately 350,000 guanine-rich sequences that can potentially form quadruplex DNA structures.[2] Some of these sequences seem to play important roles in regulating the expression of genes (among them some oncogenes such as *c-myc*[3]). On the other hand, formation of quadruplex DNA structures in the human telomere (*HTelo*) has been shown to inhibit telomerase (an enzyme overexpressed in approximately 85% of cancer cells and which plays an important role in cancer cell immortalization). Therefore, molecules that can selectively interact with quadruplex DNA and stabilize this secondary structure are receiving increasing attention as they could be potential anticancer drugs.[4−7]

Over the past 10 years a rational approach to designing small molecules that can selectively interact with quadruplex DNA has emerged.[8,9] Most of the molecules reported so far are based on planar organic heteroaromatic systems often featuring substituents that help increase the molecule's solubility and interactions with the loops and grooves of DNA.[8−10] More recently we[11−14] and others[15−21] have shown that metal

*To whom correspondence should be addressed. E-mail: r.vilar@imperial.ac.uk.

(1) Neidle, S.; Balasubramanian, S. *Quadruplex Nucleic Acids*; The Royal Society of Chemistry: Cambridge, 2006.
(2) (a) Huppert, J. L. *Biochimie* **2008**, *90*, 1140. (b) Todd, A. K.; Johnston, M.; Neidle, S. *Nucleic Acids Res.* **2005**, *33*, 2901. (c) Huppert, J. L.; Balasubramanian, S. *Nucleic Acids Res.* **2005**, *33*, 2908.
(3) Qin, Y.; Hurley, L. H. *Biochimie* **2008**, *90*, 1149.
(4) De Cian, A.; Lacroix, L.; Douarre, C.; Temime-Smaali, N.; Trentesaux, C.; Riou, J.-F.; Mergny, J.-L. *Biochimie* **2008**, *90*, 131.
(5) Ou, T.-m.; Lu, Y.-j.; Tan, J.-h.; Huang, Z.-s.; Wong, K.-Y.; Gu, L.-q. *ChemMedChem* **2008**, *3*, 690.
(6) Arola, A.; Vilar, R. *Curr. Top. Med. Chem.* **2008**, *8*, 1405.
(7) Huppert, J. L. *Philos. Trans. R. Soc., A* **2007**, *365*, 2969.
(8) Cuesta, J.; Read, M. A.; Neidle, S. *Mini-Rev. Med. Chem.* **2003**, *3*, 11.
(9) Monchaud, D.; Teulade-Fichou, M.-P. *Org. Biomol. Chem.* **2008**, *6*, 627.
(10) Neidle, S.; Parkinson, G. N. *Biochimie* **2008**, *90*, 1184.
(11) Reed, J. E.; Arnal, A. A.; Neidle, S.; Vilar, R. *J. Am. Chem. Soc.* **2006**, *128*, 5992.
(12) Reed, J. E.; Neidle, S.; Vilar, R. *Chem. Commun.* **2007**, 4366.
(13) Reed, J. E.; White, A. J. P.; Neidle, S.; Vilar, R. *Dalton Trans.* **2009**, 2558.
(14) Arola-Arnal, A.; Benet-Buchholz, J.; Neidle, S.; Vilar, R. *Inorg. Chem.* **2008**, *47*, 11910.
(15) Kieltyka, R.; Fakhoury, J.; Moitessier, N.; Sleiman, H. F. *Chem.—Eur. J.* **2008**, *14*, 1145.
(16) Bertrand, H.; Bombard, S.; Monchaud, D.; Teulade-Fichou, M.-P. *J. Biol. Inorg. Chem.* **2007**, *12*, 1003.
(17) Kieltyka, R.; Englebienne, P.; Fakhoury, J.; Autexier, C.; Moitessier, N.; Sleiman, H. F. *J. Am. Chem. Soc.* **2008**, *130*, 10040.
(18) Shi, S.; Liu, J.; Yao, T.; Geng, X.; Jiang, L.; Yang, Q.; Cheng, L.; Ji, L. *Inorg. Chem.* **2008**, *47*, 2910.
(19) Talib, J.; Green, C.; Davis, K. J.; Urathamakul, T.; Beck, J. L.; Aldrich-Wright, J. R.; Ralph, S. F. *Dalton Trans.* **2008**, 1018.
(20) Yu, H.; Wang, X.; Fu, M.; Ren, J.; Qu, X. *Nucleic Acids Res.* **2008**, *36*, 5695.
(21) Ma, D.-L.; Che, C.-M.; Yan, S.-C. *J. Am. Chem. Soc.* **2009**, *131*, 1835.

Published on Web 09/03/2009

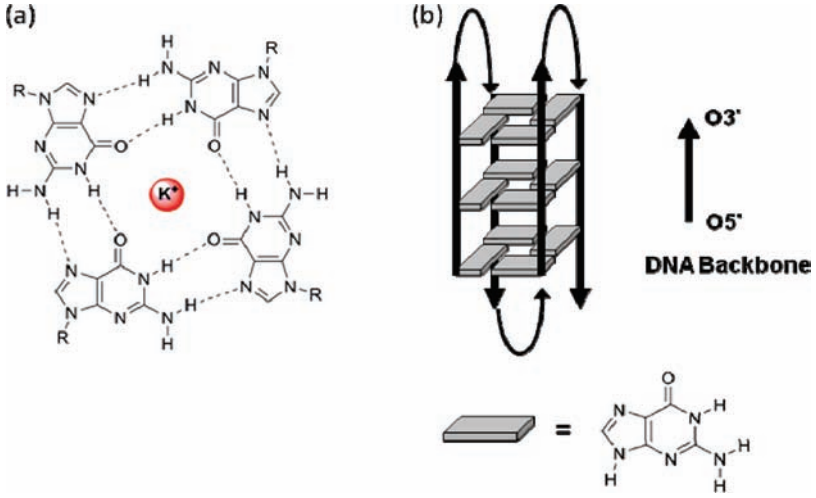

Figure 1. (a) Guanine quartet highlighting the hydrogen bonding interactions between the Watson−Crick and Hoogsteen faces of the guanine bases, and the metal cation located at the center of the quartet; (b) schematic representation of an intramolecular quadruplex DNA structure.

Scheme 1. Reaction Scheme for the Syntheses of Ligands (L^1−L^3) and Their Corresponding Platinum(II) Complexes (**1**−**3**) under Study

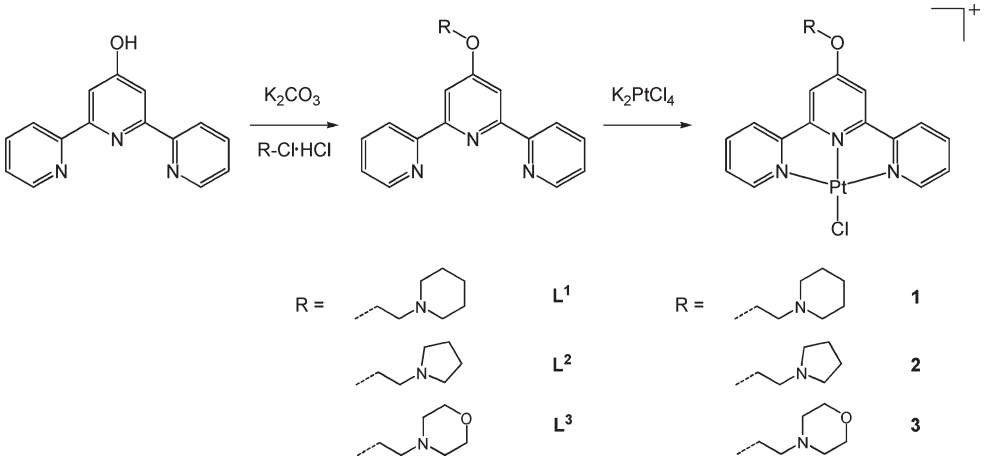

complexes can be excellent quadruplex DNA binders. The rationale behind using metal complexes in this context is based on their unique features. For example, the metal can play an important structural role in organizing ligand(s) into an optimal geometry to interact efficiently with quadruplex DNA. On the other hand, the electron-withdrawing properties of the metal reduce the electron density on the coordinated ligand and hence render a system with the ability to display strong $\pi-\pi$ interactions.[22] Finally, the electropositive metal can in principle be positioned at the center of the guanine quartet increasing electrostatic stabilization by substituting the cationic charge of the alkali metal cation that would normally occupy this site.

Herein we present the syntheses, structural characterization, and quadruplex DNA binding abilities of three new platinum(II)-terpyridine complexes. Although the interactions between metal-terpyridine complexes and DNA have been extensively studied for over 20 years,[23−29] there have been very few reports on metal-terpyridine complexes interacting with quadruplex DNA.[30] In one of these studies by Teulade-Fichou, the importance of the metal's geometry in generating good quadruplex DNA binders (with square planar terpyridine-metal complexes being the best) was shown.

As part of our ongoing interest in developing new metal complexes as quadruplex DNA binders, we decided to explore the DNA binding properties of three new terpyridine ligands and their corresponding square-planar platinum(II) complexes. As part of our design, the terpyridine ligands were functionalized with cyclic amines (see Scheme 1). These substituents have been previously shown to increase water solubility on a range of planar molecules and, on the other

(22) Janiak, C. *Dalton Trans*. **2000**, 3885.
(23) Barton, J. K.; Lippard, S. J. *Biochemistry* **1979**, *18*, 2661.
(24) Bond, P. J.; Langridge, R.; Jennette, K. W.; Lippard, S. J. *Proc. Natl. Acad. Sci. U.S.A*. **1975**, *72*, 4825.
(25) Clark, M. L.; Green, R. L.; Johnson, O. E.; Fanwick, P. E.; McMillin, D. R. *Inorg. Chem*. **2008**, *47*, 9410.
(26) Eryazici, I.; Moorefield, C. N.; Newkome, G. R. *Chem. Rev*. **2008**, *108*, 1834.
(27) Jennette, K. W.; Gill, J. T.; Sadownick, J. A.; Lippard, S. J. *J. Am. Chem. Soc*. **1976**, *98*, 6159.
(28) Peyratout, C. S.; Aldridge, T. K.; Crites, D. K.; McMillin, D. R. *Inorg. Chem*. **1995**, *34*, 4484.
(29) Yu, C.; Chan, K. H.-Y.; Wong, K. M.-C.; Yam, V. W.-W. *Proc. Natl. Acad. Sci. U.S.A*. **2006**, *103*, 19652.
(30) (a) Bertrand, H.; Monchaud, D.; De Cian, A.; Guillot, R.; Mergny, J.-L.; Teulade-Fichou, M.-P. *Org. Biomol. Chem*. **2007**, *5*, 2555. (b) Bertrand, H.; Bombard, S.; Monchaud, D.; Talbot, E.; Guedin, A.; Mergny, J. L.; Grunert, R.; Bednarski, P. J.; Teulade-Fichou, M. P. *Org. Biomol. Chem*. **2009**, *7*, 2864. (c) Bertrand, H.; Bombard, S.; Monchaud, D.; Teulade-Fichou, M.-P. *Nucleic Acids Symp. Ser*. **2008**, *52*, 163.

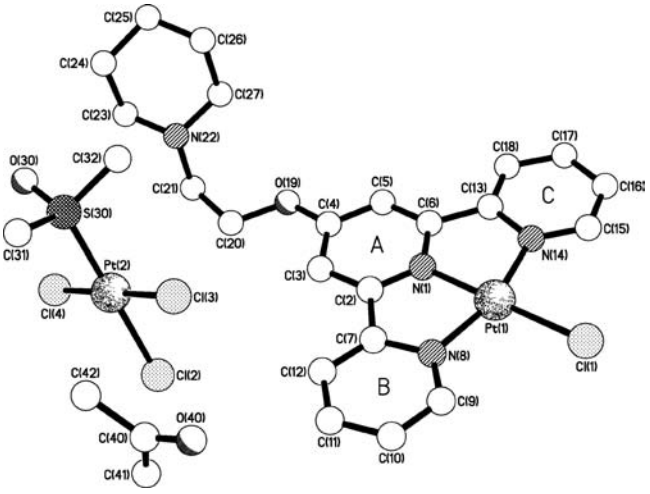

Figure 2. Molecular structure of **1**, showing the contents of the asymmetric unit.

hand, to increase their ability to interact with the loops and grooves of DNA. In addition, by including these relatively bulky substituents we aimed at reducing the ability of the terpyridine complexes to intercalate in between base-pairs of duplex DNA (an unwanted binding mode if the system is to be selective for quadruplex DNA structures). This in principle should provide a degree of selectivity if compared with unsubstituted terpyridines.

Results and Discussion

Synthesis of L^n and the Corresponding Platinum(II) Complexes $[Pt(L^n)Cl](PF_6)$. The terpyridine ligands $\mathbf{L^1}-\mathbf{L^3}$ were synthesized by reacting 2,6-bis(2-pyridyl) 4(1*H*) pyridone and the corresponding hydrochloric salt of the 1-(2-chloroethyl) cyclic amine in the presence of K_2CO_3 as a base (Scheme 1). After heating to reflux in acetone for 12 h, the reaction mixture was filtered and the solvent removed under reduced pressure. The crude solid was recrystallized with diethyl ether to yield a pure sample of the corresponding ligand. The three ligands were characterized by ^{1}H and ^{13}C NMR spectroscopy, mass spectrometry and elemental analyses (see Experimental Details).

The three new terpyridine ligands were then reacted with K_2PtCl_4 in dimethylsulfoxide (DMSO) to yield, after 15 h of heating at 50 °C, orange solutions from which solids were precipitated upon addition of acetone. To obtain pure samples of the platinum(II) complexes, the corresponding solids were redissolved in the minimum amount of DMSO and excess $NaPF_6$ (as aqueous solution) was added dropwise. This induced the exchange of counterions on the complexes yielding $[Pt(L^n)Cl](PF_6)$ (when $\mathbf{L^n} = \mathbf{L^1}$, **1**; $\mathbf{L^n} = \mathbf{L^2}$, **2**; $\mathbf{L^n} = \mathbf{L^3}$, **3**) as yellow solids.

The three platinum(II) terpyridine complexes **1**−**3** were fully characterized by ^{1}H NMR spectroscopy (which showed characteristic shifts for some of the aromatic signals upon coordination to platinum), mass spectrometry, and elemental analyses. In addition, two of the complexes were structurally characterized by X-ray crystallography.

X-ray Crystal Structures of $[Pt(L^n)Cl]Cl$ and $[Pt(L^n)Cl][PtCl_3(DMSO)]$. Crystals of **1** suitable for a single-crystal X-ray diffraction study were obtained by layering a DMSO solution of the product with acetone and left to stand for one day. The solid state structure of **1** showed the expected $[Pt(\mathbf{L^1})Cl]^+$ cation where the three pyridyl rings (A, B, and C), Pt(1), Cl(1), and O(19) are all coplanar to within about 0.07 Å (Figure 2, Table 1). This planarity allows adjacent centrosymmetrically related cations to form an extended stack (along the *a* axis direction), with the neighboring cations linked by a series of Pt···π and $\pi-\pi$ interactions (Figure 3). Interestingly, the structure revealed that under these crystallization conditions the unexpected $[PtCl_3(dmso)]^-$ complex was found as the counteranion rather than the expected chloride. This is not unprecedented when growing crystals of platinum(II) complexes from the crude reaction mixture.[31]

Table 1. Selected Bond Lengths (Å) and Angles (deg) for **1**

Pt(1)−Cl(1)	2.3056(15)	Pt(1)−N(1)	1.942(5)
Pt(1)−N(8)	2.007(6)	Pt(1)−N(14)	2.013(5)
Pt(2)−Cl(2)	2.3248(17)	Pt(2)−Cl(3)	2.2957(16)
Pt(2)−Cl(4)	2.2943(17)	Pt(2)−S(30)	2.2017(15)
N(1)−Pt(1)−N(8)	80.6(2)	N(1)−Pt(1)−N(14)	81.4(2)
N(8)−Pt(1)−N(14)	162.0(2)	Cl(1)−Pt(1)−N(1)	178.94(15)
Cl(1)−Pt(1)−N(8)	99.08(14)	Cl(1)−Pt(1)−N(14)	98.90(15)
Cl(4)−Pt(2)−S(30)	89.78(6)	Cl(3)−Pt(2)−S(30)	91.11(6)
Cl(3)−Pt(2)−Cl(4)	178.93(7)	Cl(2)−Pt(2)−S(30)	177.51(7)
Cl(2)−Pt(2)−Cl(4)	92.06(6)	Cl(2)−Pt(2)−Cl(3)	87.07(6)

The platinum atom in one cation is sandwiched between the central pyridyl ring (A) of two adjacent cations (related to the first cation by independent centers of symmetry) with Pt···π distances of about 3.56 and 3.81 Å for a and b, respectively; as a consequence of the centers of symmetry, both faces of ring A are likewise approached by platinum atoms. The vectors of the two Pt···π interactions subtend an angle of about 157° at both the platinum atom and the ring A centroid. Rings B and C π-stack with each other forming a continuous ···B···C···B···C··· array (Figure 3).

Crystals of **3** suitable for a single-crystal X-ray diffraction study were obtained by slow evaporation (over 5 days) from a DMSO solution of the product. The X-ray crystal structure of **3** revealed the presence of two crystallographically independent cations, **3-I** (Figure 4, Table 2) and **3-II** (Figure S36 in the Supporting Information), along with two chloride anions, a DMSO molecule, and three water molecules. As was seen in the structure of **1**, here in **3** for both of the independent cations, the three pyridyl rings, and the associated Pt, Cl, and O(19) atoms are coplanar to within about 0.07 Å.

Again, this planarity enables the formation of an extended stack of cations (coincidentally along the *a* axis direction again). However, the nature of interactions between the cations is noticeable different compared to **1**, reflecting a different orientation of the adjacent cations. Whereas in **1** the Pt−Cl bonds of the adjacent cations are oriented head to tail (i.e., 180°), in **3** they are orientated by about 90° (Figure 5). Additionally, in **3** the platinum centers are positioned much more closely to each other [i 3.5755(7) Å, and j 3.5579(7) Å] than was the case in **1** [where the closest Pt···Pt separation is 4.2777(5) Å]. The result in **3** is a series of $\pi-\pi$ (a, b, c and d) and Cl···π (e, f, g, h) interactions between the adjacent complexes. The centroid···centroid and mean interplanar

(31) Rochon, F. D.; Tessier, C. *Inorg. Chim. Acta* **2008**, *361*, 2591.

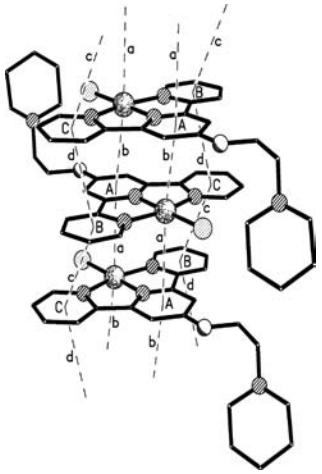

Figure 3. Part of one of the Pt···π and $\pi-\pi$ linked stacks of cations along the crystallographic *a* axis direction present in the crystals of **1**. The Pt···π distances (a) and (b) are about 3.56 and 3.81 Å, respectively, and the centroid···centroid separations for the $\pi-\pi$ contacts (c) and (d) are about 3.94 and 3.72 Å, respectively. In each case the planes of the rings are inclined by about 3°.

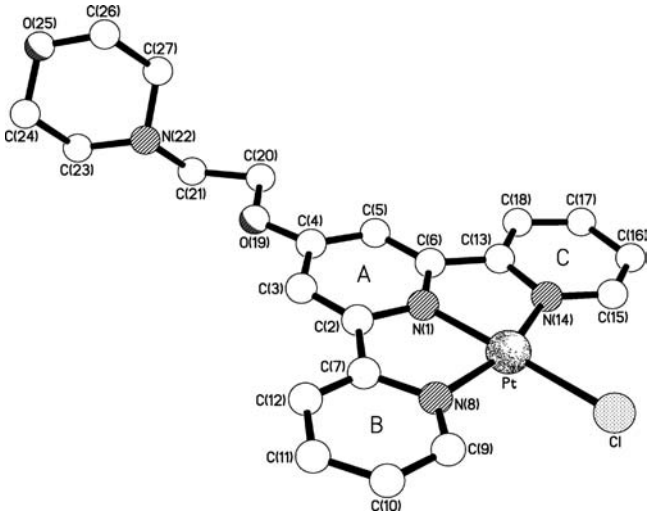

Figure 4. Molecular structure of one (**3-I**) of the two crystallographically independent cations present in the crystals of **3**.

separations (Å) for the $\pi-\pi$ interactions are (a) 3.62 and 3.37, (b) 3.62 and 3.38, (c) 3.64 and 3.38, (d) 3.60, 3.37; in each case the rings are essentially parallel (though this is not crystallographically required). For the Cl···π interactions, the Cl···π distances (Å), and the inclinations of the Cl···π vectors to the ring planes (deg) are (e) 3.44 and 80, (f) 3.58 and 71, (g) 3.46 and 78, and (h) 3.45 and 78.

Study of $\pi-\pi$ Interactions by ^{1}H NMR Spectroscopy. Having established that the platinum-terpyridine complexes display $\pi-\pi$ stacking interactions in the solid state, it was of interest to investigate whether these interactions were retained in solution. This would be relevant to establish the potential of these complexes for $\pi-\pi$ stacking with guanine quartets. ^{1}H NMR spectroscopy has been previously used to determine the degree of stacking in aromatic systems.[32,33] Molecular aggregation via $\pi-\pi$ stacking results in shielding of protons and hence in lower δ values in the ^{1}H NMR spectrum compared to the non-aggregated species. Therefore, variable temperature and variable concentration ^{1}H NMR spectroscopy can provide insight into the level of intermolecular stacking of an aromatic system. Thus, ^{1}H NMR spectra at different concentrations (2 to 14 mM) and temperatures (25 to 100 °C) were recorded in d^6-DMSO for one of the terpyridine ligands (**L^2**) and for the three metal complexes (**1**−**3**). For the free ligand, no significant changes in the ^{1}H NMR spectra were observed upon increasing the temperature or concentration (see Figures S1−S4 in the Supporting Information). This indicates that the free ligands do not display important $\pi-\pi$ interaction in solution. This is not an unexpected result since, because of the free rotation of the bond that links the terpyridyl rings, the free ligand is not planar. On the other hand, significant shifts in the resonances of the aromatic protons were observed for the terpyridine-platinum complexes upon changing the temperature or concentration of the solution. Upon increasing the temperature from 25 to a 100 °C, the resonances associated to the aromatic protons shifted to lower field (see Figure 6 below and Figures S5−S16 in the Supporting Information). This is consistent with a reduction of the intermolecular $\pi-\pi$ stacking interactions of the system at higher temperatures.

Upon increasing the concentration of the platinum complexes (i.e., favoring intermolecular $\pi-\pi$ stacking interactions), the aromatic protons shifted to lower δ values (see Figure 7 below and Figures S5−S16 in the

(32) Venkataramana, G.; Sankararaman, S. *Org. Lett.* **2006**, *8*, 2739.
(33) Nandy, R.; Subramoni, M.; Varghese, B.; Sankararaman, S. *J. Org. Chem.* **2007**, *72*, 938.

Table 2. Selected Bond Lengths (Å) and Angles (deg) for the Two Crystallographically Independent Complexes Present in the Crystals of **3**

	mol **I**	mol **II**		mol **I**	mol **II**
Pt−Cl	2.305(3)	2.306(3)	Pt−N(1)	1.945(9)	1.918(10)
Pt−N(8)	2.029(10)	2.003(9)	Pt−N(14)	1.984(9)	2.039(10)
Cl−Pt−N(1)	178.5(3)	179.2(3)	Cl−Pt−N(8)	98.4(3)	99.8(3)
Cl−Pt−N(14)	99.5(3)	98.1(3)	N(1)−Pt−N(8)	81.5(4)	81.0(4)
N(1)−Pt−N(14)	80.5(4)	81.0(4)	N(8)−Pt−N(14)	162.0(4)	162.0(4)

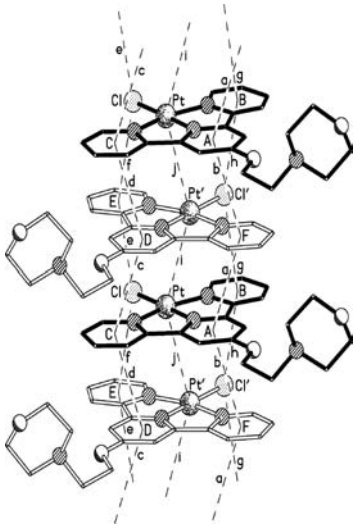

Figure 5. Part of one of the $\pi-\pi$ and Cl···π linked stacks of cations along the crystallographic *a* axis direction present in the crystals of **3** (cation **3-I** has been drawn with dark bonds, **3-II** with open bonds).

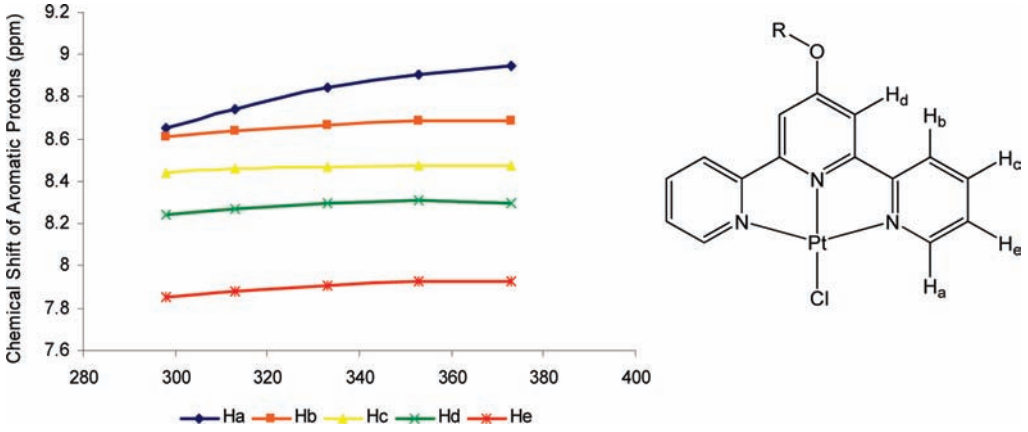

Figure 6. Plot showing the ^{1}H NMR chemical shift (of aromatic protons) vs temperature (K) for platinum complex **1**.

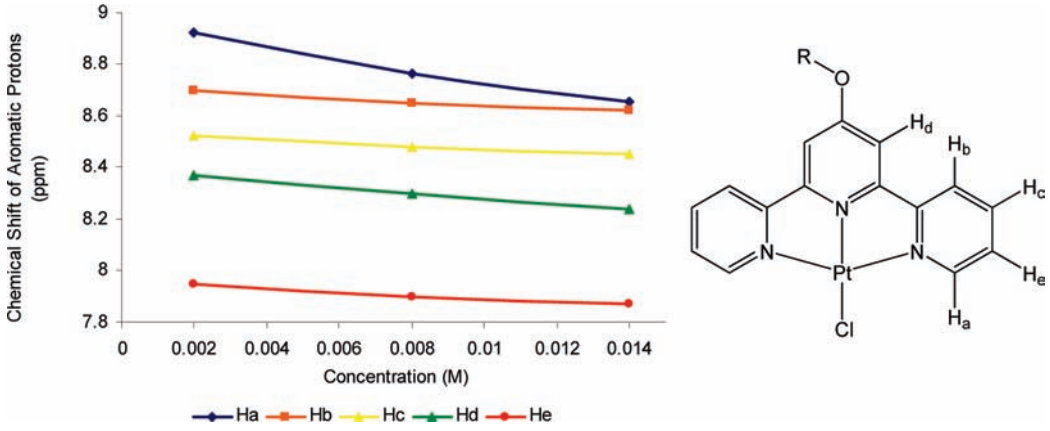

Figure 7. Plot showing the ^{1}H NMR chemical shift (of aromatic protons) vs concentration of platinum complex **1**.

Supporting Information). The variable temperature and concentration ^{1}H NMR spectroscopic studies strongly suggest that, in DMSO, the platinum-terpyridine complexes aggregate through $\pi-\pi$ interactions. Once this was established, we focused on evaluating the interactions of complexes **1**−**3** with duplex and quadruplex DNA. This was carried out using fluorescent intercalation displacement (FID) assays, surface plasmon resonance (SPR), and circular dichroism (CD).

Fluorescent Intercalator Displacement (FID) Assay. We first screened the complexes using the FID assay.[34] This recently developed technique allows for a fast semiquantitative evaluation of the DNA binding abilities of small molecules. In this method, thiazole orange (TO) is mixed with DNA with which it is known to interact strongly. When interacting with DNA, TO is luminescent; however, when free in solution the emission is quenched. Therefore, displacement of TO by another molecule provides an approximate measure of the affinity of the given compound for duplex and quadruplex DNA. To quantify the displacement, the compound's concentration at which TO fluorescence decreases by 50% (assumed to be 50% displacement of TO) is calculated ($^{G4}DC_{50}$).

We were first interested in comparing the quadruplex DNA binding abilities of the free ligands and the corresponding metal complexes. Therefore, FID studies for $\mathbf{L^1}-\mathbf{L^3}$ and complexes **1**−**3** using *HTelo* DNA were carried out. These studies showed that the platinum complexes displace TO at low μM concentrations (see $^{HTelo}DC_{50}$ values in Table 3) suggesting strong interactions between these terpyridine-platinum complexes and telomeric quadruplex DNA. In contrast, the free ligands are not able to fully displace TO even at concentrations as high at 10 μM and only 25−30% displacement at 2.5 μM (see Figure 8). This is consistent with the results obtained by ^{1}H NMR spectroscopy (see above) which indicated that the free ligands do not display any significant intermolecular $\pi-\pi$ stacking interaction (most likely because of their lack of planarity) while the corresponding square planar platinum-terpyridine complexes do.

Once the ability of the complexes to bind to telomeric DNA was established, more detailed FID studies were carried out (see figures S17−S19 in the Supporting Information for FID plots). Table 3 summarizes the DC_{50} values obtained by FID for the interactions of complexes **1**−**3** with two different quadruplex DNA sequences (*HTelo* and *c-myc*) and one duplex DNA sequence (*ds*).

The $^{cmyc}DC_{50}$ and $^{HTelo}DC_{50}$ values obtained for these complexes (particularly for **1**) are comparable to those found for other compounds reported to be good quadruplex DNA binders (see the extensive study by Teulade-Fichou[34]). However, complexes **1**−**3** show only modest binding selectivity for quadruplex vs duplex DNA (binding up to 13 times better to *c-myc* quadruplex

(34) Monchaud, D.; Allain, C.; Bertrand, H.; Smargiasso, N.; Rosu, F.; Gabelica, V.; De Cian, A.; Mergny, J. L.; Teulade-Fichou, M. P. *Biochimie* **2008**, *90*, 1207.

Table 3. $^{HTelo}DC_{50}$, $^{ds}DC_{50}$, and $^{cmyc}DC_{50}$ Values (μM) Determined Using FID Assay for Complexes **1**−**3**[a]

	TO displacement			selectivity		
complex	$^{HTelo}DC_{50}$ (μM)	$^{c\text{-}myc}DC_{50}$ (μM)	$^{ds}DC_{50}$ (μM)	$^{ds}DC_{50}/^{HTelo}DC_{50}$	$^{ds}DC_{50}/^{cmyc}DC_{50}$	$^{cmyc}DC_{50}/^{HTelo}DC_{50}$
1	1.25	0.26	3.46	2.77	13.31	4.81
2	1.44	0.42	4.11	2.85	9.79	3.43
3	2.24	1.01	4.48	2.00	4.44	2.22

[a] Values are average of three independent measurements.

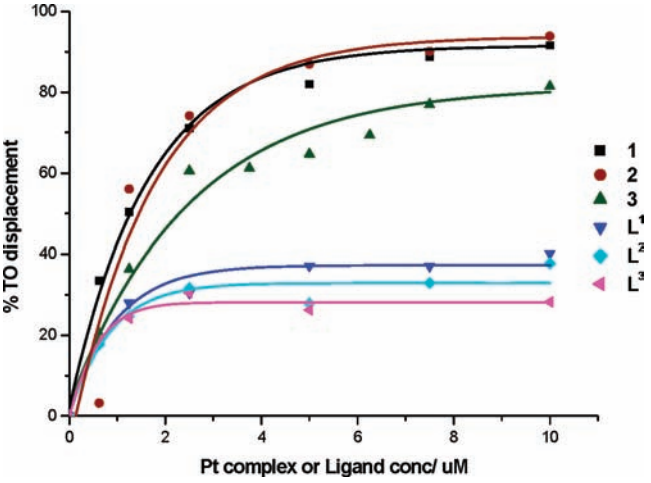

Figure 8. Graphical representation of TO displacement from human telomeric (*HTelo*) quadruplex-DNA upon increasing concentration of ligands ($\mathbf{L^1}$−$\mathbf{L^3}$) and the corresponding complexes (**1**−**3**) from 0.125 to 10 μM.

DNA than to duplex DNA). It is also worth pointing out that, although the differences are small, the complex with the morpholine substitutent (complex **3**) shows consistently higher DC_{50} values suggesting that the morpholine does not interact as strongly with the grooves and loops of DNA as the other two cyclic amine substituents.

Surface Plasmon Resonance (SPR) Studies. To obtain quantitative data for the interaction between the platinum-terpyridine complexes and quadruplex DNA sequences, surface plasmon resonance (SPR)[35] studies were carried out. The following three 5′-biotin-labeled DNA sequences were immobilized on a sensor chip via biotin-streptavidin interactions: the 22-mer human telomeric quadruplex 5′-biotin-AGGG(TTAGGG)$_3$, the 22-mer CG-rich hairpin duplex 5′-biotin-TT(CG)$_4$TTTT(CG)$_4$, and the 36-mer *c-myc* quadruplex DNA 5′-biotin-ATG-CAT-GCG-GGG-AGG-GTG-GGG-AGG-GTG-GGG-AAG-GTG-GGG. Binding experiments were carried out under salt/buffer conditions that are suitable for DNA quadruplex formation (i.e., HBS-EP buffer from BIACore supplemented with 0.2 M KCl). A range of concentrations of the corresponding complex were investigated by injecting the sample simultaneously over the three different sequences of immobilized DNA and the blank reference (flow rate of 20 μL/min; running time 5 min).

Sensorgrams were obtained for the concentration-dependent binding of complexes **1** and **2** (the two complexes with lower DC_{50} values, see above) to quadruplex/duplex DNA. From these, binding constants were calculated (see Table 4). The SPR data is consistent with these

(35) Redman, J. E. *Methods* **2007**, *43*, 302.

Table 4. Association Constants, Determined by SPR, between DNA (Htelo, *c-myc*, duplex) and Complexes **1** and **2**

compound	K_a [M^{-1}][a] *HTelo* quadruplex	K_a [M^{-1}][b] CG-rich duplex	K_a [M^{-1}][a] *c-myc* quadruplex
1	1.2×10^6	4.3×10^5	1.2×10^6
	1.5×10^5		2.3×10^4
2	1.2×10^6	4.6×10^5	1.2×10^6
	1.5×10^5		4.3×10^5

[a] Binding curves were fitted using non-equivalent two-sites binding model. This yielded two different binding constants for the interaction between the platinum complexes and quadruplex DNA. [b] Binding curves for duplex DNA were fitted using equivalent one-site binding model.

complexes binding to quadruplex DNA (both *HTelo* and *c-myc*) via a two-independent-binding-site model. The binding constant to one of the binding sites is of the order of 10^6 while the other of the order of 10^5 M^{-1}. The SPR results also show that complexes **1** and **2** bind more strongly to quadruplex than to duplex DNA (1 order of magnitude) which is consistent with the results obtained using the FID assay.

Circular Dichroism (CD) Studies with *Htelo* DNA. Human telomeric DNA can exist as a mixture of parallel and anti-parallel G-quadruplex conformations. It has been previously shown that some quadruplex DNA binders can interact preferentially with one of the two conformations.[36−38] To study whether the platinum-terpyridine complexes showed selectivity for either the parallel or the anti-parallel conformations, circular dichroism (CD) experiments were performed on mixtures of complex **1** with telomeric DNA (22AG strand 5′-AGG-GTT-AGG-GTT-AGG-GTT-AGG-G-3′). The CD spectra of *HTelo* quadruplex DNA (10 μM) displayed changes in the presence of increasing amounts of complex **1** (5−30 μM which corresponds to 0.5−3 equiv of added complex). As can be seen in Figure 9, the CD spectrum of *HTelo* DNA in Tris-HCl/KCl buffer in the absence of any binder shows two positive maxima at about 265 and 295 nm which is indicative of a mixture of anti-parallel and parallel conformations. Upon addition of increasing amounts of complex **1** to *HTelo* DNA, the band at 295 nm increases while that one at 265 nm decreases. The intensification of the 295 nm band characterizes the stabilization of the anti-parallel conformation of quadruplex DNA by **1**. At the same time, the attenuation of the 265 nm band shows the destabilization of the parallel conformation by **1**. This suggests that complex **1**, under these conditions, induces conformational changes favoring the anti-parallel conformation of *HTelo* quadruplex DNA.

(36) Zhou, J.; Yuan, G. *Chem.—Eur. J.* **2007**, *13*, 5018.
(37) Goncalves, D. P. N.; Ladame, S.; Balasubramanian, S.; Sanders, J. K. M. *Org. Biomol. Chem.* **2006**, *4*, 3337.
(38) Giraldo, R.; Suzuki, M.; Chapman, L.; Rhodes, D. *Proc. Natl. Acad. Sci. U.S.A.* **1994**, *91*, 7658.

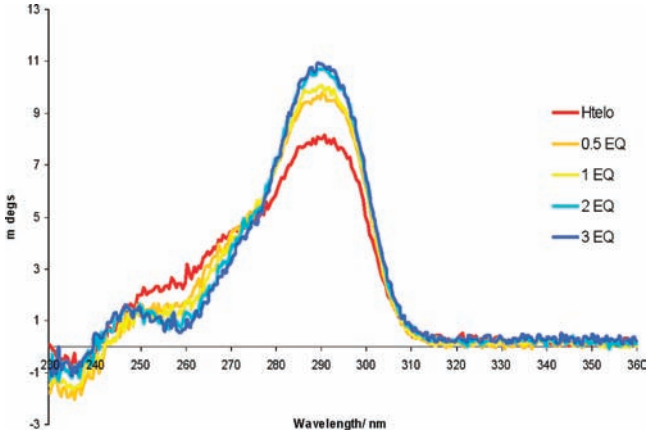

Figure 9. CD spectra of *HTelo* DNA in Tris-HCl/KCl buffer upon addition of increasing amount of complex **1** (5−30 μM, i.e. 0.5−3 eq of added complex).

Conclusions

Three new terpyiridine ligands and their corresponding platinum(II) complexes have been prepared. Two of the complexes have been structurally characterized showing that, as expected, they have a planar geometry well-suited for $\pi-\pi$ stacking interactions. Indeed, these complexes display this type of intermolecular interaction both in the solid state and in solution, as evidenced by X-ray crystallographic and ^{1}H NMR studies. This prompted us to study the potential of the complexes as quadruplex DNA binders by exploiting the interactions between the planar system of the compound and the planar guanine tetrad found in quadruplex DNA. Using FID assays, we have shown that these three complexes bind strongly to *HTelo* and *c-myc* quadruplex DNA. However, the selectivity of the complexes for quadruplex versus duplex DNA is not as high as initially expected. The incorporation of cyclic amine substituents on the terpyridines' central ring improved the solubility of the complexes in water and also the interaction with DNA. However, the initial goal that these substituents would prevent the terpyridine complexes from interacting with duplex DNA by blocking the possibility of intercalation was not fully achieved. It is likely that a second substituent is required to block the other side of the complexes from intercalation. One potential way of doing this would be by coordinating substituted thiolates or amines to the fourth position of the platinum center, which would also stop potential coordination of the platinum center to DNA. This is currently being investigated in our laboratories.

A comparison of the quadruplex DNA binding abilities of the free ligands and the corresponding metal complexes, has shown the important role played by the square planar platinum(II) center in yielding good quadruplex DNA binders. The interaction between two of these complexes (**1** and **2**) and quadruplex/duplex DNA was further investigated by SPR. These studies have confirmed that the complexes indeed bind strongly to quadruplex DNA (with constants around 10^6). The interaction with duplex DNA is 1 order of magnitude lower than with quadruplex DNA, confirming the modest selectivity observed by FID.

Experimental Details

Materials and General Procedures. All chemicals used in this study were purchased from Sigma-Aldrich Chemical Co. (except for K_2PtCl_4 which was obtained as a loan from Johnson Matthey). The purity of the organic chemicals was verified by ^{1}H NMR spectroscopy. ^{1}H NMR, ^{13}C NMR, and ^{31}P NMR spectra were recorded on a Bruker Avance 400 MHz Ultrashield NMR spectrometer. Infrared spectra were recorded on a Perkin-Elmer FTIR spectrometer. Electrospray ionization mass spectra were recorded on Bruker Daltronics Esquire 3000 spectrometer by Mr. J. Barton (Imperial College London). Elemental analyses of the compounds prepared were performed by Mr. S. Boyer (London Metropolitan University).

Synthesis of Terpyridine L^1. 2,6-Bis(2-pyridyl) 4(1*H*) pyridone (0.50 g, 2.0 mmol) and potassium carbonate (0.91 g, 6.6 mmol) were placed in acetone (25 cm^3) and heated to reflux. A solution of 1-(2-chloroethyl) piperidine hydrochloride (0.37 g, 2.0 mmol) in acetone (20 cm^3) was then added dropwise to the refluxing mixture. The mixture was heated to reflux for a further 12 h. Once cooled the potassium carbonate was filtered off, and the solvent was evaporated under reduced pressure to yield a pale yellow solid. The crude product was purified by recrystallization with diethyl ether to give **L^1** as a white solid (0.52 g, 72%); mp 94−96 °C; ^{1}H NMR (400 MHz, DMSO-d$_6$): δ_H 8.72 (d, 2H, $^3J_{HH}$ 4.0, py 2-H), 8.62 (d, 2H, $^3J_{HH}$ 8.0, py 5-H), 8.01 (dt, 2H, $^3J_{HH}$ 8.0, $^3J_{HH}$ 8.0, $^4J_{HH}$ 4.0, py 4-H), 7.98 (s, 2H, py' 3-H and 5-H), 7.51 (ddd, 2H, $^3J_{HH}$ 8.0, $^3J_{HH}$ 8.0, py 3-H), 4.34 (t, $^3J_{HH}$ 6.0, 2H, ethyl 1-H), 2.75 (t, 2H, $^3J_{HH}$ 6.0, ethyl 2-H), 2.48 (br m, 4H, piperidine 1-H), 1.63 (m, piperidine 2-H), 1.45 (m, 2H, piperidine 3-H); ^{13}C NMR (400 MHz, DMSO-d$_6$): δ_C 167.1, 157.2, 155.3, 149.7, 137.8, 125.0, 121.4, 107.3, 66.7, 57.5, 54.9, 26.1, 24.4; IR υ_{max} (cm^{-1}) 1622, 1580, 1562, 1468, 1448, 1406, 1353, 1330, 1205, 1111,1094, 1028; ESI-MS Calcd. for $C_{22}H_{24}N_4O$ [M$^+$]: 360.5 amu Found [M+H]$^+$: 361.0 a.m.u.; Anal. Calcd. for $C_{22}H_{24}N_4O$: C 73.31, H 6.71, N 15.54. Found: C 73.43, H 6.63, N 15.66.

Synthesis of Terpyridine L^2. 2,6-Bis(2-pyridyl) 4(1*H*) pyridone (0.50 g, 2.0 mmol) and potassium carbonate (0.91 g, 6.6 mmol) were placed in acetone (25 cm^3) and heated to reflux. A solution of 1-(2-chloroethyl) pyrrolidine hydrochloride (0.34 g, 2.0 mmol) in acetone (20 cm^3) was then added dropwise to the refluxing mixture. The mixture was heated to reflux for a further 12 h. Once cooled the potassium carbonate was filtered off, and the solvent was evaporated under reduced pressure to yield a pale yellow solid. The crude product was purified by recrystallization with diethyl ether to give **L^2** as an off-white solid (0.52 g, 75%); mp 82−84 °C; ^{1}H NMR (400 MHz, DMSO-d$_6$): δ_H 8.73 (d, 2H, $^3J_{HH}$ 4.0, py 2-H), 8.63 (d, 2H, $^3J_{HH}$ 8.0, py 5-H), 8.02 (dt, 2H, $^3J_{HH}$ 8.0, $^3J_{HH}$ 8.0, $^4J_{HH}$ 4.0, py 4-H), 7.98 (s, 2H, py' 3-H and 5-H), 7.51 (ddd, 2H, $^3J_{HH}$ 8.0, $^3J_{HH}$ 8.0, py 3-H), 4.36 (t, $^3J_{HH}$ 6.0, 2H, ethyl 1-H), 2.89 (t, 2H, $^3J_{HH}$ 6.0, ethyl 2-H), 2.57 (br m, 4H, pyrrolidine 1-H), 1.71 (m, pyrrolidine 2-H); ^{13}C NMR (400 MHz, DMSO-d$_6$): δ_C 167.0, 157.1, 155.3, 149.7, 137.8, 124.9, 121.3, 107.2, 67.8, 54.5, 54.4, 23.7; IR υ_{max} (cm^{-1}): 1601, 1580, 1562, 1465, 1405, 1317, 1203, 1111, 1091, 1027; ESI-MS Calcd. for $C_{21}H_{22}N_4O$ [M$^+$]: 346.4 amu Found [M+H]$^+$: 347.0 a.m.u.; Anal. Calcd. for $C_{21}H_{22}N_4O$: C 72.81, H 6.40, N 16.17. Found: C 72.69, H 6.70, N 16.10

Synthesis of Terpyridine L^3. 2,6-Bis(2-pyridyl) 4(1*H*) pyridone (0.50 g, 2.0 mmol) and potassium carbonate (0.91 g, 6.6 mmol) were placed in acetone (25 cm^3) and heated to reflux. A solution of 4-(2-chloroethyl) morpholine hydrochloride (0.37 g, 2.0 mmol) in acetone (20 cm^3) was then added dropwise to the refluxing mixture. The mixture was heated to reflux for a further 12 h. Once cooled the potassium carbonate was filtered off, and the solvent was evaporated under reduced pressure to yield a pale yellow solid. The crude product was purified by recrystallization with diethyl ether to give **L^2** as an off-white solid (0.53 g, 73%); mp 80−82 °C; ^{1}H NMR (400 MHz, DMSO-d$_6$): δ_H 8.72 (d, 2H, $^3J_{HH}$ 4.0, py 2-H), 8.61 (d, 2H, $^3J_{HH}$ 8.0, py 5-H), 8.00 (dt, 2H, $^3J_{HH}$ 8.0, $^3J_{HH}$ 8.0, $^4J_{HH}$ 4.0, py 4-H), 7.97 (s, 2H, py' 3-H and 5-H), 7.50 (ddd, 2H, $^3J_{HH}$ 8.0, $^3J_{HH}$ 8.0, py 3-H), 4.36 (t, $^3J_{HH}$ 6.0, 2H, ethyl 1-H), 3.59 (m, 4H, morpholine 1-H), 2.78

Table 5. Crystallographic Data for Compounds **1** and **3**[a]

data	**1**	**3**
chemical formula	$[C_{22}H_{24}ClN_4OPt]$ $(C_2H_6OSCl_3Pt)$	$[C_{21}H_{22}ClN_4O_2Pt](Cl)$
solvent	Me_2CO	$0.5Me_2SO \cdot 1.5H_2O$
fw	1028.64	694.50
T (°C)	−100	−100
space group	$P2_1/n$ (No. 14)	$P2_1/c$ (No. 14)
a (Å)	7.2194(2)	6.8187(2)
b (Å)	18.4980(5)	26.9591(12)
c (Å)	24.3290(8)	26.5291(9)
α (deg)		
β (deg)	91.323(2)	91.100(3)
γ (deg)		
V (Å^3)	3248.14(16)	4875.8(3)
Z	4	8 [b]
D_{calcd} (g cm^{-3})	2.103	1.673
λ (Å)	1.54184	1.54184 [c]
μ (mm^{-1})	19.800	13.498
R_1[c]	0.0299	0.0681
wR_2[d]	0.0685	0.1048

[a] Oxford Diffraction Xcalibur PX Ultra diffractometer, Cu Kα radiation, refinement based on F^2. [b] There are two independent molecules. [c] $R_1 = \sum||F_o| - |F_c||/\sum|F_o|$. [d] $wR_2 = \{\sum w(F_o^2 - F_c^2)^2/\sum w(F_o^2)^2\}^{1/2}$; $w^{-1} = \sigma^2(F_o^2) + (aP)^2 + bP$.

(t, 2H, $^3J_{HH}$ 6.0, ethyl 2-H), 2.52 (m, 4H, morpholine 2-H); ^{13}C NMR (400 MHz, DMSO-d$_6$): δ_C 167.0, 157.1, 155.3, 149.7, 137.8, 125.0, 121.4, 107.3, 66.7, 66.4, 57.2, 54.1; IR υ_{max} (cm^{-1}): 1598, 1580, 1559, 1469, 1445, 1403, 1354, 1324, 1306, 1146, 1111, 1024; ESI-MS Calcd. for $C_{21}H_{22}N_4O_2$ [M$^+$]: 362.4 amu Found [M+H]$^+$: 363.0 a.m.u.; Anal. Calcd. for $C_{21}H_{22}N_4O_2$: C 69.59, H 6.12, N 15.46. Found: C 69.50, H 6.14, N 15.41

Synthesis of Complex [Pt(L^1)Cl](PF$_6$) (1). K_2PtCl_4 (0.29 g, 0.7 mmol) was added to DMSO (15 cm^3) at 50 °C. To this, a solution of **L^1** (0.25 g, 0.7 mmol) in DMSO (30 cm^3) was added dropwise, and the resulting mixture was stirred for 15 h to yield a deep orange solution. The solution was then added dropwise to acetone (ca. 100 cm^3) and an orange solid precipitated. The product was isolated by filtration and repeatedly washed with acetone. This solid was dissolved in the minimum amount of DMSO, to which an excess $NaPF_6$ (as an aqueous solution) was added dropwise. The resultant yellow precipitate was isolated by filtration and washed repeatedly with water, methanol, and diethyl ether. The yellow solid was dried under reduced pressure to yield [Pt(**L^1**)Cl](PF$_6$) (0.13 g, 25%). ^{1}H NMR (400 MHz, DMSO-d$_6$): δ_H 8.98 (br d, 2H, $^3J_{HH}$ 4.0, py 2-H), 8.69 (br d, 2H, $^3J_{HH}$ 8.0, py 5-H), 8.57 (br dt, 2H, $^3J_{HH}$ 8.0, $^3J_{HH}$ 6.0, py 4-H), 8.36 (br s, 2H, py' 3-H and 5-H), 7.99 (br t, 2H, $^3J_{HH}$ 8.0, py 3-H), 4.74 (br s, 2H, ethyl 1-H); ^{31}P NMR (400 MHz, DMSO-d$_6$): δ_P −144.22 (sept, 1P, $^1J_{PF}$ 1756, PF$_6$); Anal. Calcd. for $C_{22}H_{24}N_4OClPF_6Pt$: C 35.90, H 3.29, N 7.61. Found: C 35.83, H 3.14, N 7.51

Synthesis of Complex [Pt(L^2)Cl](PF$_6$) (2). K_2PtCl_4 (0.30 g, 0.7 mmol) was added to DMSO (15 cm^3) at 50 °C. To this, a solution of **L^2** (0.25 g, 0.7 mmol) in DMSO (30 cm^3) was added dropwise, and the resulting mixture was stirred for 15 h to yield a deep orange solution. The solution was then added dropwise to acetone (ca. 100 cm^3), and a yellow solid precipitated. The product was isolated by filtration and repeatedly washed with acetone. This solid was dissolved in the minimum amount of DMSO, to which an excess of $NaPF_6$ (as an aqueous solution) was added dropwise. The resultant yellow precipitate was isolated by filtration and washed repeatedly with water, methanol, and diethyl ether. The yellow solid was dried under reduced pressure to yield [Pt(**L^2**)Cl](PF$_6$) (0.08 g, 15%). ^{1}H NMR (400 MHz, DMSO-d$_6$): δ_H 9.00 (br d, 2H, $^3J_{HH}$ 8.0, py 2-H), 8.70 (br d, 2H, $^3J_{HH}$ 8.0, py 5-H), 8.57 (br dt, 2H, $^3J_{HH}$ 8.0, $^3J_{HH}$ 6.0, py 4-H), 8.37 (br s, 2H, py' 3-H and 5-H), 8.00 (br t, 2H, $^3J_{HH}$ 6.0, py 3-H), 4.71 (br s, 2H, ethyl 1-H); ^{31}P NMR (400 MHz, DMSO-d$_6$): δ_P −144.21 (sept, 1P, $^1J_{PF}$ 1756, PF$_6$); ESI-MS Calcd. for $C_{21}H_{22}N_4OClPF_6Pt$ [M$^+$]: 721.1 amu Found [M+H]$^+$: 721.0 a.m.u.; Anal. Calcd. for $C_{21}H_{22}N_4OClPF_6Pt$: C 34.94, H 3.07, N 7.76. Found: C 34.85, H 2.98, N 7.65

Synthesis of Complex [Pt(L^3)Cl](PF$_6$) (3). K_2PtCl_4 (0.29 g, 0.7 mmol) was added to DMSO (15 cm^3) at 50 °C. To this, a solution of **L^3** (0.25 g, 0.7 mmol) in DMSO (30 cm^3) was added dropwise, and the resulting mixture was stirred for 15 h to yield a deep orange solution. The solution was then added dropwise to acetone (ca. 100 cm^3), and a yellow solid precipitated. The product was isolated by filtration and repeatedly washed with acetone. This solid was dissolved in the minimum amount of DMSO, to which an excess of $NaPF_6$ (as an aqueous solution) was added dropwise. The resultant yellow precipitate was isolated by filtration and washed repeatedly with water, methanol, and diethyl ether. The yellow solid was dried under reduced pressure to yield [Pt(**L^3**)Cl](PF$_6$) (0.15 g, 30%). ^{1}H NMR (400 MHz, DMSO-d$_6$): δ_H 8.99 (br d, 2H, $^3J_{HH}$ 4.0, py 2-H), 8.69 (br d, 2H, $^3J_{HH}$ 8.0, py 5-H), 8.56 (br dt, 2H, $^3J_{HH}$ 8.0, $^3J_{HH}$ 6.0, py 4-H), 8.35 (br s, 2H, py' 3-H and 5-H), 7.99 (br t, 2H, $^3J_{HH}$ 8.0, py 3-H), 4.74 (br s, 2H, ethyl 1-H); ^{31}P NMR (400 MHz, DMSO-d$_6$): δ_P −144.59 (sept, 1P, $^1J_{PF}$ 1752, PF$_6$); ESI-MS Calcd. for $C_{21}H_{22}N_4O_2ClPF_6Pt$ [M$^+$]: 737.1 amu Found [M+H]$^+$: 737.0 a.m.u.; Anal. Calcd. for $C_{21}H_{22}N_4O_2ClPF_6Pt$: C 34.18, H 3.00, N 7.59. Found: C 34.05, H 2.93, N 7.43

X-ray Crystallography. Table 5 provides a summary of the crystallographic data for compounds **1** and **3**. Data for **1**: Collected at 173 K, pale yellow needles; 5082 independent measured reflections, F^2 refinement, $R_1 = 0.030$, $wR_2 = 0.069$, 3988 independent observed absorption-corrected reflections [$|F_o| > 4\sigma(|F_o|)$, $2\theta_{max} = 126°$], 372 parameters. CCDC 739341. Data for **3**: Collected at 173 K, yellow needles; 9265 independent measured reflections, F^2 refinement, $R_1 = 0.068$, $wR_2 = 0.105$, 5015 independent observed absorption-corrected reflections [$|F_o| > 4\sigma(|F_o|)$, $2\theta_{max} = 143°$], 604 parameters. CCDC 739342.

Variable Temperature and Variable Concentration ^{1}H NMR Spectroscopic Studies. The ^{1}H NMR spectroscopic studies were all carried out in DMSO-d$_6$. For the variable concentration ^{1}H NMR studies three different concentrations were used: 0.002 M, 0.008, and 0.014 M. The variable temperature ^{1}H NMR studies were conducted on a Bruker Avance 500 MHz Ultrashield NMR spectrometer at 293, 313, 323, 333, 353, 373, 393, 413, and 433 K.

Oligonucleotide Preparation for FID Assay. All the oligonucleotides used were purchased from Eurogentec S.A. (U.K.). The 22AG strand (5′-AGG-GTT-AGG-GTT-AGG-GTT-AGG-G-3′) and 20AG strand (5′-GG-GAG-GGT-GGG-GAG-GGT-GGG-3′) were used for the human telomeric and

c-myc studies, respectively. For the duplex DNA studies a 17 base-pair complementary strand was used (5′-GGG-TTA-CTA-CGA-ACT-GG-3′ with 5′-CCA-GTT-CGT-AGT-AAC-CC-3′). The oligonucleotides were dissolved in Milli Q water to yield a 20 μM stock solution. This was then diluted using 10 mM potassium cacodylate (pH 7.4)/50 mM potassium chloride (60 mM K^+) buffer to the appropriate concentrations. Prior to use in the FID assay, the DNA strands were annealed by heating to 95 °C for 5 min and then by cooling to room temperature overnight.

Sample Preparation for FID Assay. The platinum complexes (**1**−**3**), ligands ($\mathbf{L^1}$−$\mathbf{L^3}$) and thiazole orange (TO) were dissolved in DMSO to give 1 mM stock solutions. The corresponding solution was then diluted using 10 mM potassium cacodylate (pH 7.4)/50 mM potassium chloride (60 mM K^+) buffer to the appropriate concentrations.

FID Assay Procedure. The FID assay was carried out as previously reported.[34] To a mixture of DNA sequence (0.25 μM) and TO (0.50 μM) in 10 mM potassium cacodylate (pH 7.4)/ 50 mM potassium chloride (60 mM K^+) buffer an increasing amount of the corresponding molecule under study (platinum complex or terpyridine ligand) was added (0.125 to 10 μM, which corresponds to 0.5 to 40 equiv). After an equilibration time of 3 min the emission spectrum was recorded between 510 and 750 nm with an excitation wavelength of 501 nm. This was recorded using a Varian Cary Eclipse Spectrometer. The fluorescence area was calculated using the "trapezium rule" method. The area was converted into percentage TO displacement by the following formula: % TO displacement = 100 − [(fluorescence area of sample/fluorescence area of standard) × 100]. The standard fluorescence spectrum was obtained in the absence of any molecule. % TO displacement was then plotted against each of the compound concentrations to give the respective FID curves.

Oligonucleotide Preparation for SPR Studies. Biotinylated oligonucleotides were used for the SPR experiments. As with the FID studies, all the oligonucleotides used were purchased from Eurogentec S.A. (U.K.). The 22AG strand (5′-biotin-AGG-GTT-AGG-GTT-AGG-GTT-AGG-G-3′) and 39AG strand (5′-biotin-ATG-CAT-GCG-GGG-AGG-GTG-GGG-AGG-GTG-GGG-AAG-GTG-GGG-3′) were used for the human telomeric and *c-myc* studies, respectively. For the duplex DNA studies the 22 CG-rich strand (5′-biotin-TTC-GCG-CGC-GTT-TTC-GCG-CGC-G-3′) was used. Prior to immobilizing the biotinylated oligonucleotides onto the SPR chip, the respective strands were dissolved in Milli Q water to form a 20 μM stock solution. This was then diluted further to 10 nM using HBS-EP buffer (0.01 M HEPES pH 7.4, 0.15 M NaCl, 3 mM EDTA,0.005% v/v Surfactant P20) purchased from GE Healthcare U.K. Ltd., supplemented with degassed 0.2 M KCl solution. The DNA strands were then annealed by heating to 95 °C for 5 min and then cooling slowly to room temperature.

Sample Preparation for SPR Studies. The corresponding platinum complex (**1** or **2**) was dissolved in DMSO to yield a 1 mM stock solution. This was then diluted using HBS-EP/KCl buffer to the appropriate concentrations. Seven millimeter glass vials with pierceable plastic caps (purchased from Sigma Aldrich) were used to contain the platinum complex solutions during the SPR experiment.

SPR Procedure. The SPR experiments were carried out on the four-channel BIACore 3000 optical biosensor instrument using previously published methods.[35] The oligonucleotides were loaded onto a streptavidin-coated four-flow cell sensorchips (SA) purchased from GE Healthcare U.K. Ltd. As part of the preparatory steps the sensorchip was conditioned with injections of 1 M NaCl in 50 mM NaOH followed by prolonged washings with buffer. Three of the four flow cells were loaded with the respective labeled DNA strands by manual injection of the 10 nM oligonucleotide solutions (preparation details given above) at a flow rate of 2 μL/min for 7 min. This was sufficient to achieve RU levels of about 600 RU. The last flow cell was left blank as a reference. Once the oligonucleotides were immobilized onto the sensorchip, the SPR experiments were conducted in running HBS-EP/KCl buffer by multiple injections of a range of Pt complex concentrations (analyte), 0−2 μM. Each analyte concentration was passed over the four flow cells for 5 min at a flow rate of 20 μL/min. Between injections the original sensorchip surface was regenerated by running buffer. To obtain the true sensorgrams corresponding to each of the platinum complex concentrations, each sensorgram was subtracted from the reference. To determine the binding constants of the Pt complexes with the respective DNA sequences, the sensorgrams were analyzed using BIAevaluation 4.0.1. The response in the steady-state region (R_{eq}) was found by linear averaging over a 50 s time span. The response was then converted to r, moles of bound compound per mole of DNA (see Supporting Information for details of the calculations).

Oligonucleotide Preparation for CD Studies. All oligonucleotides used were purchased from Eurogentec S.A. (U.K.). The 22AG human telomeric DNA strand (5′-AGG-GTT-AGG-GTT-AGG-GTT-AGG-G-3′) was used. The oligonucleotides were dissolved in Milli Q water to yield a 100 μM stock solution. This was then diluted using 50 mM Tris-HCl (pH 7.4)/150 mM KCl buffer to 20 μM. Prior to use in the CD assay, the DNA solution was annealed by heating to 95 °C for 5 min and then by cooling to room temperature.

Sample Preparation for CD Studies. Complex **1** was dissolved in DMSO to yield a 1 mM stock solution. This was then diluted using Tris-HCl/KCl buffer to the appropriate concentrations.

CD Measurements. The CD spectra were recorded in a strain-free 10 mm × 2 mm rectangular cell path length cuvette. The data was obtained on an Applied Photophysics Ltd. Chirascan spectrometer. The CD spectra were measured in the wavelength region of 700−180 nm with the following parameters: bandwidth, 1 nm; spectral range, 230−360 nm; step-size, 0.5 nm; time-pep-point, 1.5 s. The CD spectra were collected and analyzed using the Chirascan and Chirascan Viewer softwares, respectively. A titration was carried out for the *HTelo* sequence in KCl buffer. The CD spectra were recorded for oligonucleotide/complex **1** solutions with 0.5, 1, 2, and 3 ratios. For each solution mixture the oligonucleotide final concentration was maintained at 10 μM.

Acknowledgment. The Engineering and Physical Sciences Research Council, U.K., is thanked for a studentship to K.S., and Johnson Matthey PLC for a generous loan of platinum.

Supporting Information Available: Variable temperature and variable concentration ^{1}H NMR spectra. Plots for FID and SPR studies. Details for the analysis of the SPR data. X-ray crystallographic data and CIF files. This material is available free of charge via the Internet at http://pubs.acs.org. Structures have been deposited with the Cambridge Crystallographic Data Centre (http://www.ccdc.cam.ac.uk; CCDC numbers: 739341 and 739342).